NovoViz

Beyond sensing

Investigation of photon counting statistics in a coherent state by leveraging a SPAD-based photon number resolver

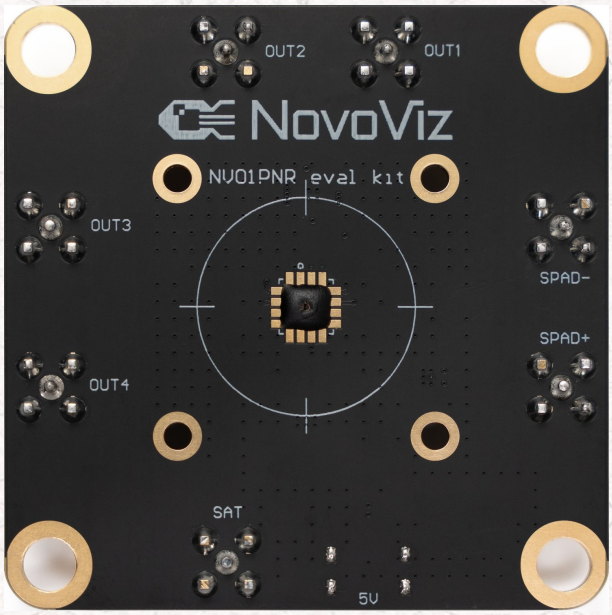

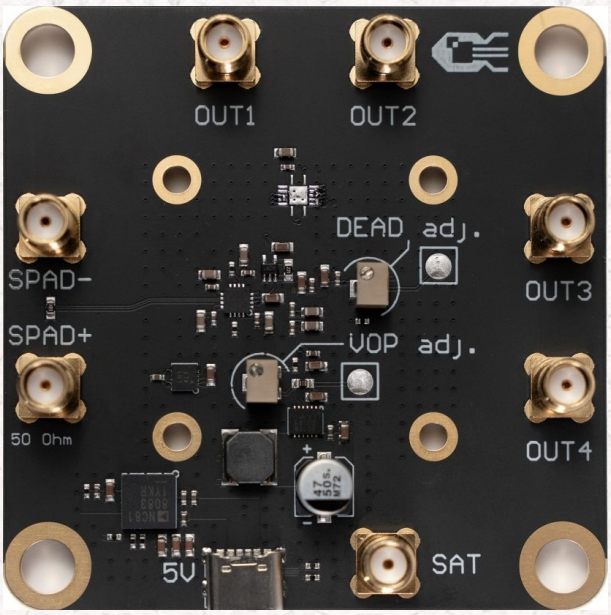

Introduction

Photon-number resolvers (PNRs) are crucial in quantum optics, quantum communication, quantum computing, and metrology, as they accurately determine the number of photons present in an incident light beam—an essential capability when working with non-Gaussian light sources. The ability to resolve photon numbers in light pulses or quantum states of light is critical in:

1

Metrology of light sources
to distinguish between thermal, coherent, or single-photon light, and assessing the purity and efficiency of quantum light sources,

2

Quantum imaging
to enhance sensitivity and signal-to-noise ratio (SNR), and allowing high resolution imaging beyond classical limits,

3

Quantum communication
to enable the use of higher-dimensional quantum states, which support higher key rates and faster quantum key distribution systems,

4

Quantum state analysis
to identify non-classical light states such as entangled, squeezed, and Fock states, and preparing states with pre-defined photon number.

Most PNR detectors today are based on superconducting technologies, primarily superconducting nanowire single-photon detectors (SNSPDs) and transition-edge sensors (TESs). In SNSPD-based systems, photon-number information can be extracted from characteristics of the electrical output signal or by using multiple detector elements in parallel to distinguish simultaneous photon arrivals, enabling fast operation and high sensitivity [1]. TES-based detectors, on the other hand, determine photon numbers by measuring changes in electrical resistance caused by absorbed photon energy, offering excellent accuracy but relying on inherently slower thermal processes [2]. Despite their strong performance, these superconducting PNR technologies come with significant practical limitations. They require cryogenic cooling, which increases system complexity, cost, and power consumption, and makes integration into compact or scalable systems challenging.

As an alternative to superconducting PNR detectors, single-photon avalanche diodes (SPADs) offer a compelling solution due to their ability to operate at room or near-room temperature, eliminating the need for complex cryogenic cooling. However, resolving more than one photon with a single SPAD device remains challenging, as SPADs exhibit a certain dead time before registering a subsequent photon hit. This limitation can be addressed by arranging an array of SPADs to spatially cover the incoming light beam, with photon-number resolution determined by the number of elements in the array. In this work, we present NovoViz's compact PNR module, NV01PNR-DEV, based on a 4×4 SPAD array that combines high sensitivity with fast, configurable timing electronics. Using a coherent pulsed laser source, we demonstrate accurate reconstruction of Poissonian photon statistics, validating the module's capability as a practical, scalable, and non-cryogenic alternative to superconducting detectors.

Theory

In coherent-state light sources, photon-emission statistics follow a Poisson distribution. Accordingly, the probability of detecting n photons, $P(n)$, is given by:

$$P(n) = e^{-\langle n \rangle} \frac{\langle n \rangle^n}{n!}, \tag{1}$$

where $\langle n \rangle$ denotes the mean photon number, i.e., the expected value of the photon number in the state [3]. In principle, the Poissonian behavior of coherent states can be verified using a pulsed laser (a coherent source) together with a PNR. For different values of $\langle n \rangle$, the photon number n can be measured with a PNR under each condition. The measured distribution of n can then be compared with the theoretical $P(n)$ calculated from the corresponding $\langle n \rangle$. Such plots reveal whether the measured photon-number distribution follows Poissonian statistics. As the optical power increases, a shift of the distribution peak toward higher photon numbers is also expected.

To conduct these measurements, the experimental setup used in this work is shown in Figure 1. A 405 nm pulsed laser (PicoQuant LDH-D-C-405 laser head, controlled by a PDL 800-D laser driver) was coupled to a collimator. The 405 nm wavelength was chosen because it lies close

to the peak sensitivity (~ 450 nm) of the SPADs integrated in the PNR module. The collimated laser beam was directed by a mirror through absorptive neutral density filters to reduce the optical power to the low-light regime. It then passed through an optical diffuser to evenly distribute the light and decrease its spatial coherence across the SPAD cluster. Finally, the PNR module was connected to a Swabian Instruments time tagger, which recorded the average photon count per second (cps).

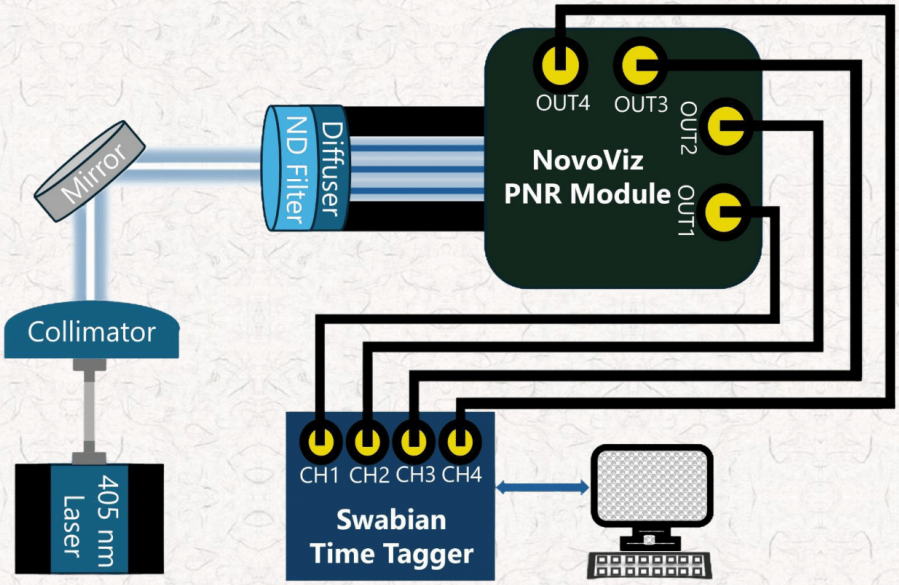

Figure 1. Schematic of the optical setup used to characterize the SPAD-based PNR with a coherent pulsed laser

NovoViz's PNR product is based on a 4×4 SPAD array with a 28 μm pixel pitch. Each SPAD has a 10 μm diameter sensitive area. The peak detection probability is around the 450 nm wavelength, reaching 20% and 35% at an excess bias voltage (V_{ex}) of 1 volt and 3 volts. The system generates a digital pulse from four individual outputs corresponding to the simultaneous detection of at least one (OUT1), two (OUT2), three (OUT3), or four photons (OUT4) on the SPAD cluster. Each SPAD in the cluster has its own associated active recharge circuit, which allows the dead time of the SPAD detection (T_{dead}) to be set on-board via a potentiometer-controlled external voltage pin. T_{dead} can be adjusted between 2.5 ns and 8 ns. If the detection events of individual SPADs occur within this T_{dead} time window, they are considered coincident. A summary of the NovoViz PNR module specifications and its operating principle are illustrated in Table 1 and in Figure 2.

Table 1. NovoViz PNR module's specifications.

SPAD cluster	Pixel pitch	Sensitive area	Detection probability	T_{dead}	OUT1, OUT2, OUT3, OUT4
4×4	28 μm	10 μm diameter for each SPAD	20 - 35% at 1 - 3 V_{ex}, 450 nm (peak)	2.5 - 8 ns	≥ 1, ≥ 2, ≥ 3, ≥ 4 photon(s) detected

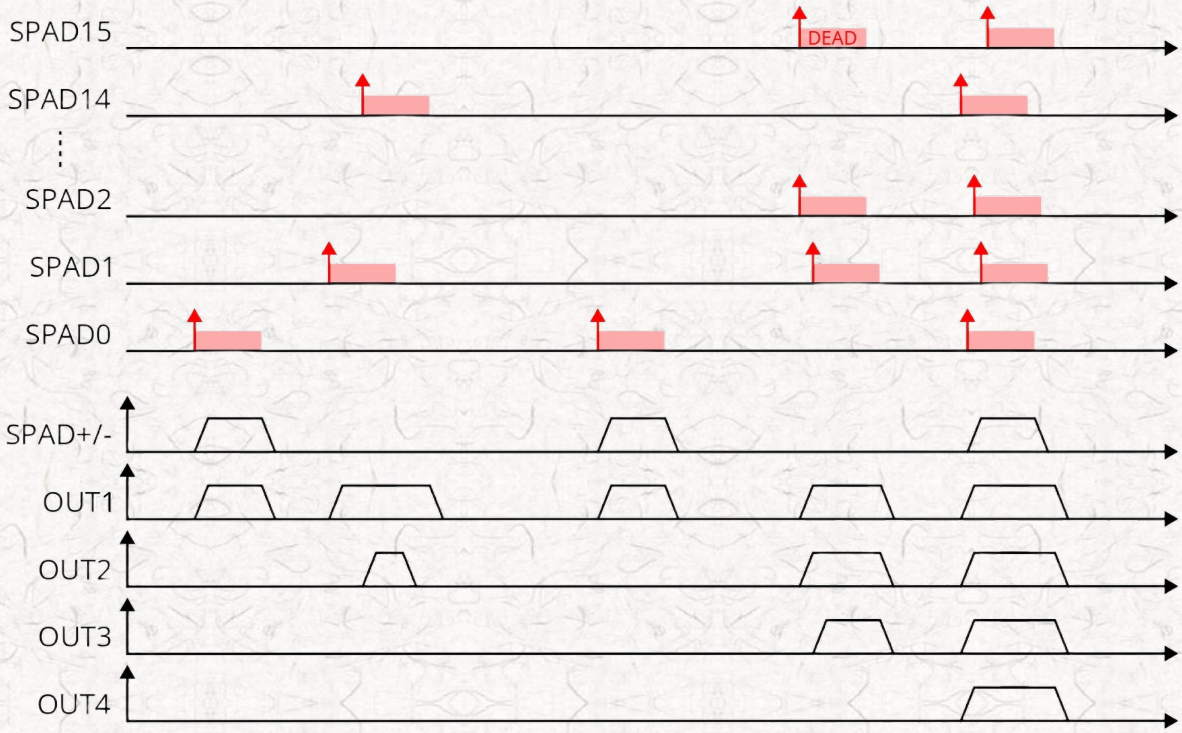

Figure 2. A representative timing diagram of the PNR

By leveraging the PNR features, the exact detected photon number of 1 during one second of laser illumination ($n_{1,cps}$) can be calculated by subtracting the OUT2 count rate and the OUT1 dark count rate (DCR) from the OUT1 count rate, as follows:

$$n_{1,cps} = OUT1_{cps} - OUT2_{cps} - OUT1_{DCR}. \quad (2)$$

As explained, OUTx corresponds to the detection of at least x photons, which necessitates this subtraction operation. DCR refers to the total number of detections per second at OUTx under complete darkness. In a similar manner, the detected photon numbers of 2 ($n_{2,\mathrm{cps}}$) and 3 ($n_{3,\mathrm{cps}}$) in one second are computed as:

$$n_{2,\mathrm{cps}} = OUT2_{\mathrm{cps}} - OUT3_{\mathrm{cps}} - OUT2_{\mathrm{DCR}}, \tag{3}$$

$$n_{3,\mathrm{cps}} = OUT3_{\mathrm{cps}} - OUT4_{\mathrm{cps}} - OUT3_{\mathrm{DCR}}. \tag{4}$$

The count rate of OUT4 remains unchanged, representing in fact $n_{\geq 4,\mathrm{cps}}$ rather than $n_{4,\mathrm{cps}}$. The zero-detection rate, $n_{0,\mathrm{cps}}$, is then calculated as:

$$n_{0,\mathrm{cps}} = f - (n_{1,\mathrm{cps}} + n_{2,\mathrm{cps}} + n_{3,\mathrm{cps}} + n_{\geq 4,\mathrm{cps}}), \tag{5}$$

where f denotes the laser repetition frequency, based on the fact that a photon detection can occur only once during each laser period. Afterwards, to convert the detected photon numbers into a probability distribution function (PDF), each $n_{\mathrm{x,cps}}$ is normalized by f:

$$P(n = x) = \frac{n_{\mathrm{x,cps}}}{f}. \tag{6}$$

The mean number of photons, $\langle n \rangle$, can then be extracted either with:

$$\langle n \rangle = -\ln(P(0)), \tag{7}$$

from Equation 1 or from the expected value of the PDF as:

$$\langle n \rangle = \sum_{x=0}^{\infty} xP(x). \tag{8}$$

Since $n = 4,5$, and higher photon numbers cannot be distinguished with this PNR module, Equation 7 is used to obtain a correct Poisson curve fit. Finally, plotting the Poisson distribution with the mean photon number $\langle n \rangle$, that is derived from the measurements, together with the measured PDF, reveals whether the photon statistics of the pulsed laser indeed follow a Poisson distribution.

Experimental Results

The DCRs of each output channel of the SPAD cluster were first measured with T_{dead} = 4 ns. At room temperature and 1 V_{ex}, the DCRs of OUT1–OUT4 were 1700, 1.7, 0, and 0 cps, respectively. Under this configuration, the typical afterpulsing probability of a single SPAD was approximately 1%. Subsequently, the photon count rates of OUT1–OUT4 were recorded under four different illumination conditions, at the same V_{ex}. In each case, the optical power was varied by adjusting either the tuning value or the laser frequency from the laser controller.

Based on the formulation presented in the theory section and the recorded OUTx count values from the PNR, a mean photon number of $\langle n \rangle = 0.29$ was obtained for the first illumination, corresponding to the lowest input power level in this experiment. Figure 3 illustrates the corresponding PDF of this measurement along with the Poisson distribution calculated using the acquired $\langle n \rangle$. As shown, the PDF closely follows the Poisson distribution, confirming the coherent nature of the pulsed laser source for $\langle n \rangle = 0.29$.

In the succeeding cases, the laser power was gradually increased, yielding $\langle n \rangle = 0.69$, $\langle n \rangle = 1.14$, and $\langle n \rangle = 2.72$. For $\langle n \rangle = 0.69$ and 1.14, the photon statistics again matched the Poisson distribution well, as depicted in Figures 4 and 5. For $\langle n \rangle = 2.72$, however, slight deviations at $\langle n \rangle = 1$ and $\langle n \rangle = 2$ became more noticeable as the mean photon number increased, which can be observed in Figure 6. This divergence can be attributed to secondary pulse-generation mechanisms, such as afterpulsing and crosstalk, which introduce false counts, as well as hot pixels that might be present in the cluster, causing non-idealities. Nonetheless, since $P(n = 3)$ nearly coincides with the Poisson fit, the fitted Poisson distribution can still be used to reasonably estimate higher-order probabilities, $P(n \geq 4)$, even though the PNR cannot directly resolve these photon numbers. For example, at $\langle n \rangle = 2.72$, one can expect approximate probabilities of $P(n = 4) \approx 0.15$, $P(n = 5) \approx 0.08$, $P(n = 6) \approx 0.037$, and $P(n = 7) \approx 0.014$.

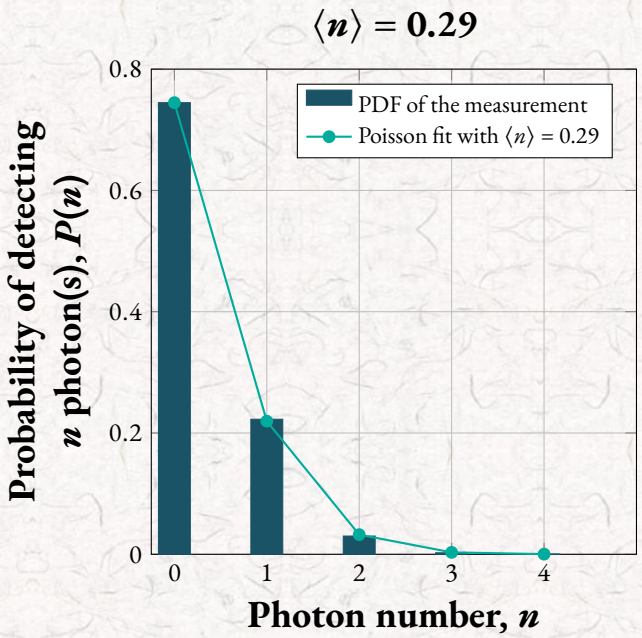

Figure 3. Acquired PDF and Poisson fit for $\langle n \rangle = 0.29$ illumination level.

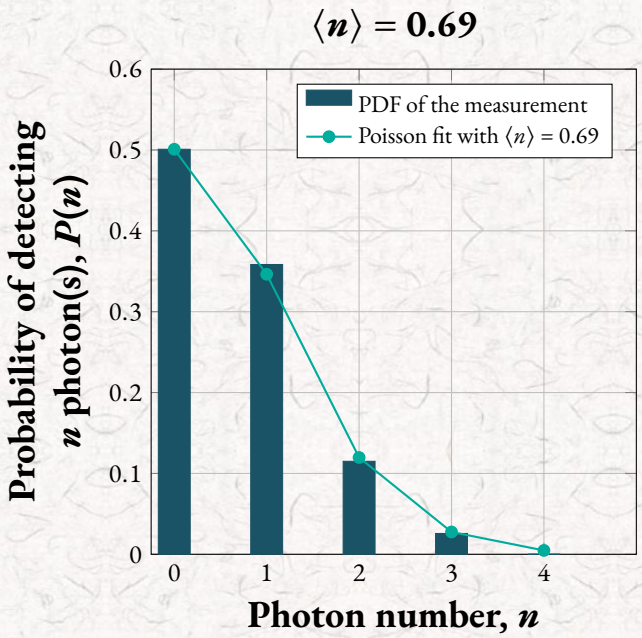

Figure 4. Acquired PDF and Poisson fit for $\langle n \rangle = 0.69$ illumination level.

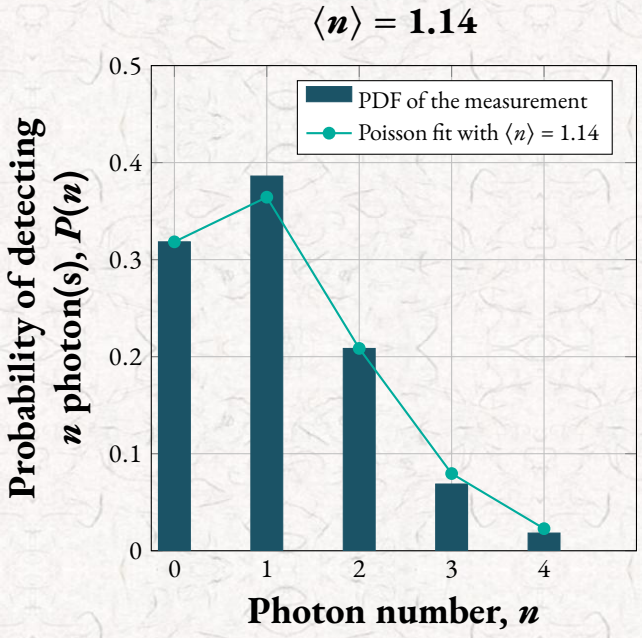

Figure 5. Acquired PDF and Poisson fit for $\langle n \rangle = 1.14$ illumination level.

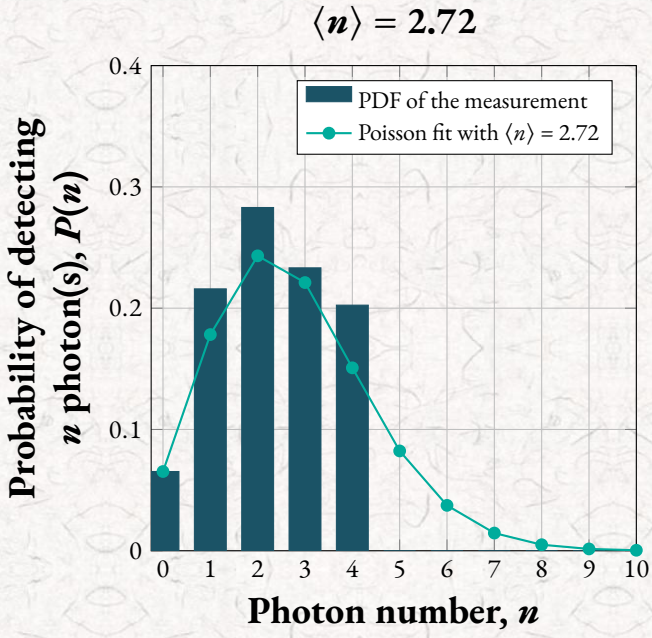

Figure 6. Acquired PDF and Poisson fit for $\langle n \rangle = 2.72$ illumination level.

Conclusion

Our experiments confirm that the NovoViz NV01PNR-DEV SPAD-based photon-number resolver operates with low noise, adjustable dead time, and high temporal resolution, delivering performance that aligns with theoretical photon statistics while operating entirely at room temperature. This result is more than a proof of principle; it represents a shift from fragile, cryogenic photon-number resolvers toward compact, deployable photon-counting modules. By demonstrating that a 4×4 SPAD cluster can reliably resolve photon-number distributions, we establish a pathway toward larger arrays and more sophisticated architectures. To place the proposed SPAD-based PNR in context, Table 2 summarizes a high-level comparison between the presented module and commonly used superconducting PNR technologies.

Table 2. Comparison of PNR technologies.

Feature	**SPAD-based NovoViz PNR (4×4)**	**SNSPD-based**	**TES-based**
Photon-number resolution	Limited by array size	High	Very high
Operating temperature	Room temperature	Cryogenic (~ 2 - 4 K)	Cryogenic (~ 100 mK)
System cost/complexity	Low	High	Very high
Scalability/integration	High (CMOS-compatible)	Limited	Very limited
Timing resolution	ns scale (configurable)	ps scale	μs-ms scale

Looking forward, SPAD-based PNRs can unlock new opportunities in several areas:

- Quantum communication: scalable integration into quantum key distribution systems;
- Quantum optics research: portable photon-statistics measurements without cryogenics;
- Advanced sensing and metrology: increased sensitivity and accessibility for laboratory and field-deployed systems.

References

1. Hadfield, R. H. "Single-photon detectors for optical quantum information applications." Nature photonics 3.12 (2009): 696-705.
2. Eisaman, M. D., et al. "Invited review article: Single-photon sources and detectors." Review of scientific instruments 82.7 (2011).
3. Fox, A. M. “Quantum optics: an introduction.” Vol. 15. Oxford university press, 2006.

Author

Utku Karaca is a pixel engineer and co-founder at NovoViz SA, specializing in CMOS and III-V SPAD sensor design and single-photon imaging. He received his BS and MS degrees in electrical and electronics engineering from Middle East Technical University, Turkey, in 2016 and 2018, and his PhD degree in microelectronics from EPFL, Switzerland, in 2024. From 2016 to 2018, he worked as research engineer at the Quantum Devices and Nanophotonics Laboratory, focusing on the design, fabrication, and characterization of III-V infrared sensor arrays. During his PhD at the Advanced Quantum Architecture Laboratory, he developed novel CMOS and III-V SPAD pixel architectures and arrays for improved photon detection at near- and short-wave infrared wavelengths. His current research centers on compact, high-speed photon-counting systems and cameras enabling precise optical measurements and imaging under low-light conditions.

E-Mail: utku.karaca@novoviz.com
Phone: +43 676 620 7707

For any inquiries, please refer to the web page below or the QR code.
https://novoviz.com/photon-number-resolver/